# Effect of Fluidization on Catalytic Cumene Dealkylation

**J. F. MATHIS and C. C. WATSON,** University of Wisconsin, Madison, Wisconsin

**This paper reports a direct experimental comparison of the cracking of cumene in a fluidized bed of silica-alumina catalyst with the same reaction in a fixed bed. The effects of fluidization on the kinetics of this reaction are interpreted in terms of an empirical approach using effectiveness factors and by a simplified mathematical model.**

A great deal of work has been done to determine the nature of flow in the fluidized bed (*7, 8, 9, 11, 12, 13, 21, 22*). The character of the fluidization obtained with liquid-solid beds has been described as uniform, or *particulate*, as opposed to the nonuniform, or *aggregative*, nature of fluidized gas-solids systems which are considered here. Bed uniformity has been defined (*13*) as the absence of gross concentration and flow discontinuities in the bed. Gas-solids fluidized beds generally exhibit nonuniformity at all velocities above the minimum fluidization velocity. In such a system most of the gas passes through the bed in pockets or bubbles which collectively form a disperse phase, and the remainder of the bed constitutes the dense phase. These bubbles are not bounded by a free surface as in the case of gas bubbles in a liquid and consequently do not retain their original identity of composition in passage through the bed. The passage of the disperse phase through the bed sets up local and over-all solids and gas-circulation patterns (*7, 8, 9*). At lower velocities all or a portion of the bed may channel or bridge; at high rates slugging may occur.

Some work has been done to obtain a quantitative measurement of bed uniformity. Morse and Ballou (*14*), Gerald (*6*), and Shuster and Kisliak (*19*) have devised separate, ingenious methods of determining bed uniformity, but in their studies uniformity was presented as some empirical function of the specific experimental results and no general interpretation of the possible effects of uniformity on the results of solid-gas reactions in a fluidized bed was made. In these studies the gas velocity, bed height, and tube diameter (or related variables) served to correlate the uniformity data for a given solid and fluid.

Gilliland and Mason and coworkers (*7* to *9*) have studied the extent of gas and solid mixing and gas by-passing in fluidized beds in a series of experiments including gas tracer studies, gas residence-time studies, heat transfer studies, and kinetic studies of a gas-phase homogeneous reaction. These experiments indicated that the effect of longitudinal gas mixing in the small-diameter fluidized bed was secondary to the effects of gas by-passing; for example, in the homogeneous reaction data, the fact that actual conversions fell considerably below those obtained in a packed bed or the empty tube was attributed to gas by-passing.

Askins, Hinds, and Kunreuther (*1*) found extensive recirculation of gas in a commercial fluid catalyst regenerator, but their data also indicate a considerable degree of gas by-passing in bubbles.

Danckwerts, Jenkins, and Place (*5*) concluded from using helium as a tracer in a commercial fluid-catalyst regenerator that the gas flow in the bed was much closer to piston flow than to complete mixing. They attributed the extent of mixing which was reported by Askins, et al. to the latter having sampled disproportionately from the dense phase in the bed. Their own exit samples were taken from the stack, after the cyclones.

A number of studies of reaction kinetics in fluidized beds have been reported in the literature, but except for the recent work of Shen and Johnstone (*23*) the intrinsic effects of fluidization on the kinetics of heterogeneous reactions in solid-gas reactions in fluidized beds have not been reported. Shen and Johnstone's studies are discussed in a later section. Interpretation of most of the available work is hampered from this standpoint because comparable fixed-bed data were not obtained; a further difficulty encountered in some of the earlier work was that the unproved assumption of progressive or piston flow (such as occurs in fixed beds) was used to integrate the rate equations developed. Another assumption which has been suggested as a basis for predicting the results of gas-solids reactions in fluidized beds is that of complete gas mixing. However, as Gilliland, Mason, and Oliver (*9*) and others have pointed out, the gas flow pattern in the fluidized bed apparently does not bear out this assumption even though in some cases a fairly close match with experimental results is obtained.

## KINETICS EXPERIMENTS

The reaction chosen for investigating the effect of fluidization on apparent reaction mechanism was the catalytic dealkylation of cumene (isopropyl benzene). This reaction was chosen because it had desirable experimental qualities and has been investigated thoroughly by Garver (*3*) and Rase (*15*), who determined that a single-site surface-reaction mechanism was followed in fixed-bed experiments.

The feed stock used in the experiments was technical-grade cumene obtained from the Dow Chemical Company, purified by distillation on a thirty-plate Oldershaw column operated at a 10 to 1 reflux ratio.

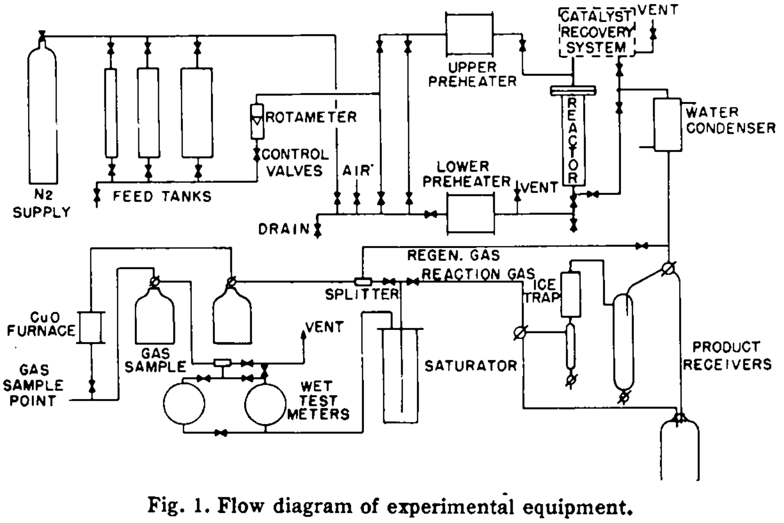

Fig. 1. Flow diagram of experimental equipment.

---

J. F. Mathis is with the Humble Oil and Refining Company, Baytown, Texas.

Tabular material has been deposited as document 5053 with the American Documentation Institute Photoduplication Service, Library of Congress, Washington 25, D. C., and may be obtained for $1.25 for photoprints or 35-mm. microfilm.

The catalyst used in the studies was the 100- to 200-mesh fraction of a fresh, ground commercial silica-alumina cracking catalyst furnished by the Universal Oil Products Company. The catalyst had a bulk density of from 0.54 to 0.59 g./cc. and a particle density of 1.2 g./cc. The screened catalyst was normally heated at 105°C. to equilibrium dryness before being charged to the system.

A flow diagram of the experimental system is given in Figure 1. The equipment can be divided functionally into the feed system, the reaction system, and the product-recovery system. Included in the feed system are three tanks of 1-, 5-, and 20-liter capacity, nitrogen supply for pressuring the feed tanks and for process purposes, feed control valves and rotameter, and various nitrogen and feed lines. The reaction system contains upper and lower preheaters, a reactor, a catalyst-recovery system, and transfer lines. The product-recovery system comprises the water-cooled condenser, liquid-product receivers, ice-water condenser and trap, gas saturator, wet-test meters, gas-sampling bottles, copper oxide furnace, and gas-sampling manifold. All equipment, lines, and fittings operating in excess of 400°F. were constructed of type-304 stainless steel.

For the fluidized runs three electrically heated, interchangeable reactors of 2-, 3-, and 4-in. standard pipe size were used. Each reactor was approximately 21 in. high and fitted with a 200-mesh support screen and backing plate at the bottom. The backing plates were perforated with 1/16-in. holes on ¼-in. centers. Feed was charged to the lower preheater and flowed up through the reactor in the fluidized operations. A cyclone separator and screen filter mounted above the reactor were used to recover the catalyst entrained in the product stream. The recovered catalyst was returned to the reactor through a motor-driven valve. Periodic injection of nitrogen into the rotary valve was used to offset the occasional tendency of the catalyst to pack in the bottom section of the cyclone.

In the fixed-bed studies a thin catalyst bed, 3⅝ in. in diameter and ¼ in. deep, located in a special "sandwich" insert in the 4-in. reactor was employed. About 20 g. of catalyst were placed in the insert between two porous micrometallic stainless steel plates. For fixed-bed operations feed was passed through the upper preheater, and in downflow through the reactor, and the catalyst-recovery system was blanked off. The temperature of the bed was measured by a multiple-junction stainless steel/chromel thermocouple inserted directly in the bed. This special couple was used to minimize undesirable side reactions promoted by the more common thermocouple compositions which lead to erroneous temperature measurements.

In all operations the feed rate was determined from the timed change in feed-tank levels, which were calibrated in terms of liquid volume. Static pressures were obtained from mercury manometers or pressure gauges. Gas flows were measured by two 20 cu. ft./hr. wet-test meters operated singly or in parallel. Process temperatures were registered on an automatic recorder from readings of iron-constantan thermocouples located at various positions in the equipment. Feed rates and temperatures were controlled manually. In general, a standard procedure was followed in all runs. This procedure was developed from preliminary experiments to give reproducible results and to ensure that a steady state and constant catalyst activity was approximated during the sampling period. Prior to a set of runs the required amount of catalyst was charged to the reactor, and the various heater settings were adjusted to give the desired lined-out temperatures. Before each run a 30-min. nitrogen pretreatment was employed to purge the system of regeneration gases and to condition the catalyst. After pretreatment feed was charged to the reactor at the prescribed rate. Timing of the run was started at the instant gas flow occurred, an indication that the reactant had contacted the catalyst. The reaction was allowed to proceed for 40 min. to permit the system to achieve a steady state of conversion, pressure, temperature, and recovery; during this time the liquid product went to the waste-product receiver. The gas and liquid samples characterizing the run were started at the 40-min. mark and were usually taken over the next 20-min. period. At the end of the sampling period the liquid product stream was again switched to waste, the gas sample stopped, and the feed valves shut off. Regeneration of the catalyst with air followed a nitrogen purge and was continued until essentially complete, as denoted by the return of the bed temperatures to their original values following the initial rise. Maximum bed temperatures were held to 1,150°F. to prevent catalyst deactivation. During regeneration a sample of the off gas was taken for analysis.

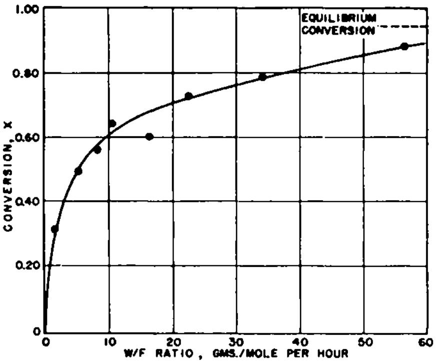

Fig. 2. Conversion as a function of *W/F* for fixed-bed operation (down flow) in the 4-in. reactor at 1 atm. and 950°F.

Samples of liquid-run product, process gas, and regeneration gas were analyzed. The benzene and cumene in the liquid product were determined by distillation in a spinner microstill developed by the Sinclair laboratories. The molecular weight and unsaturated content of the gaseous-run product were obtained by differential weighing of a sample bulb and by absorption in fuming sulfuric acid. The regeneration gas was analyzed for carbon dioxide content (after first having been passed through the copper oxide furnace to convert carbon monoxide to carbon dioxide) in a modified Orsat apparatus where the carbon dioxide was absorbed in a 33% potassium hydroxide solution.

The primary dependent variable obtained from the run data was the cumene conversion, but material balances and yield data were also developed. The calculation of the material balance and yield data (weight percentage on feed) for a given sampling period followed directly from the run data and analytical results except for calculation of the amount of the coke, which of course was deposited and measured for the entire run instead of the sampling period only. The amount of carbon formed was shown in auxiliary experiments to be proportional to the square root of the elapsed process time, and this fact and the assumption of 10 wt. % hydrogen in the coke were used to convert the measured carbon yields to coke yields for any desired process period. In a few of the fluidized runs in the 3- and 4-in. reactors at the high feed rates the reactor pressures exceeded 1.0 atm. by appreciable amounts because of the large frictional pressure drop in the product lines at large flow rates. The conversions from these runs at higher pressures were corrected to atmospheric-pressure conditions by use of pressure-correction factors based on the mechanism developed from the fixed-bed data. This correction was generally less than 10% of the experimental conversion.

The major independent variables used in the correlations were the reciprocal space velocity or *W/F* ratio, the superficial gas velocity, and the *L/D* ratio. The *W/F* ratio is the weight of catalyst in grams divided by the feed rate in gram moles per hour. The average velocity was computed from the reactor temperature, pressure, size, and feed rate, with the increase in the number of moles allowed for as the reaction proceeds. The bed height for calculation of the *L/D* ratio was determined from the temperature traverses but could be checked from a correlation of bed density and velocity developed in independent experiments.

## RESULTS

Separate reproducibility studies demonstrated that no change in catalyst activity took place over five operating cycles when standard operating procedure was used. Runs in the empty 4-in. reactor indicated that the contribution of thermal or wall reaction to the total conversion at run conditions was negligible.

### Fixed-bed Runs

The series of fixed-bed runs was made with 21.8 g. of catalyst in the bed, a reactor pressure of 1.0 atm., and a bed temperature of 950°F. The relation between the experimental conversion and the *W/F* ratio is given in Figure 2. The value of the equilibrium conversion at reaction conditions is 0.94 according to calculation from Bureau of Standards thermodynamic data (*2*). The experimental conversions appear to approach the equilibrium values very slowly in the higher *W/F* range, and this may indicate strong adsorption of a primary reaction product on the catalyst or fouling of the catalyst with secondary reaction products. The effect of process time on the fixed-bed reaction was not developed to resolve these possibilities, but on the basis of more complete data, Rase (*15, 16*) has suggested that surface fouling may be responsible for the observed conversion pattern.

Rase (*15, 16*) and Garver (*3, 4*) investigated the dealkylation of cumene over a bead-type silica-alumina catalyst in fixed beds. Their results indicated that the over-all reaction rate is controlled by a single-site surface reaction, and it was also possible to fit the results of the present fixed-bed study with this mechanism. The values of the constants in the rate equation for the present data were in agreement with those from the other studies with the exception of an unusually high value of the product adsorption equilibrium constant obtained in the present case, which might be expected as the present study covered a much greater *W/F* range than the others and the depression of the conversion, which might indicate a more strongly adsorbed product, was more marked in the higher *W/F* ranges.

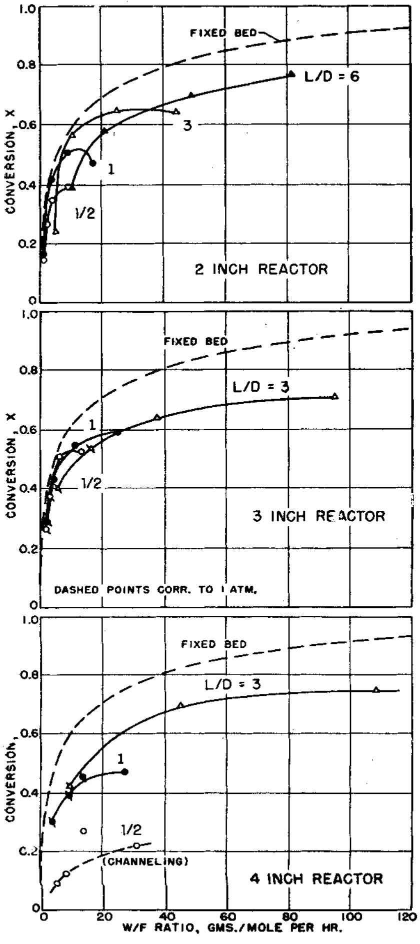

**Fig. 3. Conversion as a function of *W/F* for fluidized operation (up flow), solid lines, compared with fixed-bed operation, broken lines, at 1 atm. and 950°F.**

### Fluidized Runs

The fluidized runs were made in the 2-, 3-, and 4-in. reactors operating at 1 atm. and 950°F. These experiments were designed to cover a range of values of the velocity and bed *L/D* ratio, which had been determined in the photographic studies to be factors influencing bed uniformity. Velocities ranged from 0.05 to 0.8 ft./sec., and *L/D* varied from ½ to 6. The feed rates and weights of catalyst used were those required to give the desired velocities and *L/D* ratios.

The effect of fluidization on the results of kinetics studies in the various reactors can be seen in the plots of conversion as a function of *W/F* in Figure 3. In all cases the conversions from fluidized operation are equal to or less than those from the fixed-bed studies. The data clearly indicate the importance of the *L/D* and velocity in determining conversion from the fluidized operations, and they further suggest that the reactor diameter influences the final conversion. These effects are segregated in Figure 4, which compares the conversion data for a given *L/D* and reactor diameter from fluidized runs with the corresponding fixed-bed results for the same *W/F* ratio. Figure 4 suggests that an optimum velocity exists for the closest approach of the fluidized conversion to the fixed-bed result, which is between 0.3 and 0.5 ft./sec. for the system investigated. Figure 4 also shows that the optimum is less well defined as the *L/D* or reactor size increases but that the magnitude of the minimum spread between the two conversions increases as either *L/D* or reactor size is increased independently. This observation indicates that the reactor diameter must be specified as well as the *L/D* and velocity to define the conversion from fluidized operation with respect to the fixed-bed result. The unusually low conversions observed in a few of the fluidized runs obtained in the 4-in. reactor were probably the result of channeling in the wide beds operating at the low *L/D* and velocity conditions.

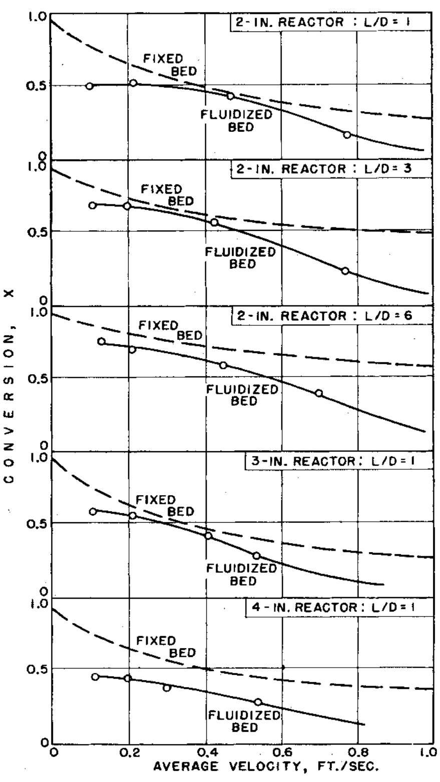

**Fig. 4. Conversion as a function of average gas velocity in fluidized operation, compared with corresponding fixed-bed conversions at the same *W/F* ratio.**

The experimental results may be explained by qualitative examination of the actions of a fluidized bed of catalyst, which might be compared with those of the identical bed in downflow.

As the rate of flow of gas upward through the catalyst bed is increased from zero, the following events take place.

1. At flow rates below the minimum fluidization rate, the operation is identical with that of a bed in downflow; it is fixed-bed operation.

2. As the flow rate is increased slightly past the minimum fluidization rate,

*a.* The bed begins to be fluidized. This condition is inherently one of nonuniformity, with some of the gas flowing upward through a dense phase at substantially the minimum fluidization velocity, while the remainder of the gas passes up through the bed in streams of bubbles. When the bed is in a fluidized condition, all the particles undergo continuous agitation, either in the dense phase or light phase. The gas flowing in the streams of bubbles is, in effect, by-passing the bulk of the catalyst.

*b.* At relatively low gas velocities, channeling rather than fluidization may take place in all or part of the bed. When a bed is channeling, most of the gas is blowing through holes in a settled, or bridged, layer of particles. Some of the gas may be flowing through this settled layer, but there is no continual agitation of the particles.

Both the by-passing of gas in a normally fluidized bed and the channeling in a poorly fluidized bed will tend to be harmful to the conversion, and to the selectivity, where competing side reactions are possible.

It may well be that if channeling could be avoided, and a bed kept normally fluidized, a gradual departure from fixed-bed performance would be observed, as gas flow rate was increased. This might require some sort of mechanical agitation, to prevent bridging and settling of the particles. However, the results of the present work suggest that channeling does tend to occur, with large departures from fixed-bed performance, for low gas rates.

3. As gas velocity is further increased, significant recirculation of catalyst will get underway, which may in general be harmful to both conversion and selectivity.

4. Continued increase in gas velocity brings about a corrective action in the turbulent intermixing between the dense and light phases, which limits the nonuniformity of gas and catalyst composition and thus tends to bring the conversion closer to that for the fixed-bed operation again.

The experimental results indicate that there is indeed a range of gas velocity where there is a minimum departure of fluidized- from fixed-bed conversion. Comparison with the findings of other experimenters (*18*, *19*) indicates qualitatively similar results. Such behavior is not unlike that observed in bubble-plate fractionation, where the local efficiency goes through a maximum as vapor velocity is increased and for some of the same reasons as in the present case.

### Fluidization-effectiveness Factors

The effect of fluidization on the apparent mechanism can be put into a more compact form through the use of fluidization-effectiveness factors, which are defined by analogy with the diffusional-effectiveness factor for catalyst pellets (*20*) as the ratio of the $W/F$ required for a given fixed-bed operation to that required for a fluidized operation at the same conversion level. Effectiveness factors derived from the experimental data are given in Figure 5. $E_f$ tends to go through a maximum value at the optimum gas velocity, and in general the maximum $E_f$ value decreases as either the $L/D$ or reactor diameter is increased independently.

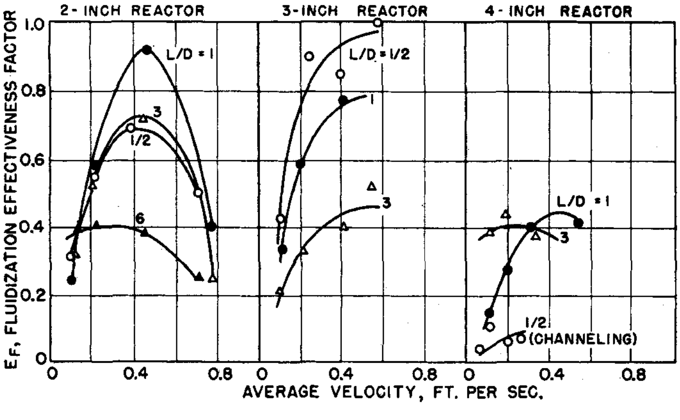

Fig. 5. Fluidization effectiveness factor as a function of average gas velocity.

### FLUIDIZED REACTOR MODEL

It is possible to develop an approximate model of fluidized-bed behavior by reference to the flow behavior in the bed. The purpose of such a development is to aid in the understanding of the effects of fluidization on reaction kinetics. In the present model the fluidized reactor is assumed to be split into parallel components corresponding to the disperse and dense phases. The total feed stream and the total weight of catalyst are assumed to be distributed between the two reactors. Progressive gas flow in both sections and constant pressure and catalyst temperature conditions are assumed throughout the bed. Any improvement in conversion over that realized in the separate phases acting independently is covered by introducing a pseudo mass transfer contribution formally based on the film theory of mass transfer but in reality a convenient mathematical starting point which directionally may approximate the actual mechanisms of conversion improvement in the bed. To simplify the development the additional assumption of pseudo-first-order kinetics is made. This assumption is not so restrictive as may be thought on first consideration because a great many catalytic reactions can be fitted with the first-order mechanism if the rate constant is taken as an empirical function of either conversion or reciprocal space velocity. The use of a more complicated mechanism is not warranted because of the limitations of the other assumptions.

Figure 6 illustrates the development. In the volume element $(A_A \Delta Z)$ of phase $A$, which can represent either the dense or disperse phase, the reactant concentration is the quantity $(1 - x_A)$ where $x$ is the conversion per unit mass of feed charged. For steady state conditions a material balance of the reactant over the volume element is as follows:

*Input*

1. Feed in
   $N_1$(moles per unit time) $= F_A(1 - x_A)$
2. Reactant transferred from phase $B$
   $N_2 = (K_{AB}A)[(1 - x_B) - (1 - x_A)]\Delta Z$
   where
   $K_{AB}$ is the interaction coefficient, moles per unit time per unit volume of bed per unit concentration difference between the $A$ and $B$ phases.
   $A$ is the total reactor cross-sectional area.
   $Z$ is the distance from the inlet.

*Output*

1. Feed out
   $N_3 = F_A[1 - (x_A + \Delta x_A)]$
2. Reaction
   $N_4 = r \cdot \Delta W_A$
   where
   $r$ is the reaction rate, moles reacted per unit time per mass of catalyst.
   $\Delta W_A$ is the mass of catalyst in the incremental volume.

Equating the input and output, passing to the differentiation limit, and simplifying gives

$$F_A\, dx_A + (K_{AB}A)(x_A - x_B)\, dZ = r \cdot dW_A \quad (1)$$

For the pseudo-first-order reaction,

$$r = k - k'x_A \quad (2)$$

where

$k' = k/x^*$.

$k$ is the pseudo-first-order rate constant, gram moles per hour per gram of catalyst.

$x^*$ is the equilibrium conversion.

The amount of catalyst in the incremental section is given by

$$dW_A = A_A \rho_A\, dZ = H_A\, dZ \quad (3)$$

where

$H_A = A_A \rho_A$, the catalyst loading factor or mass of catalyst per unit length of the reactor in phase $A$.

Equations (2) and (3) are substituted into Equation (1); after rearrangement the following first-order differential equation is obtained:

$$\frac{dx_A}{dZ} + \left[\frac{(K_{AB}A) + H_A k'}{F_A}\right] x_A - \frac{(K_{AB}A)}{F_A} x_B = \frac{H_A k}{F_A} \quad (4)$$

A similar balance for the reactant in a differential element in the $B$ phase yields a companion equation to Equation (4):

$$\frac{dx_B}{dZ} - \frac{(K_{AB}A)}{F_B}x_A + \left[\frac{(K_{AB}A) + H_Bk'}{F_B}\right]x_B = \frac{H_Bk}{F_B} \quad (5)$$

Equations (4) and (5) form a system of simultaneous ordinary first-order differential equations which can be readily solved by use of the assumptions of progressive gas flow, constant temperature and pressure, and constant average catalyst loading factors in each phase individually. The boundary condition is

$$x_A = x_B = 0 \quad \text{when} \quad Z = 0.$$

The integrated conversions for each phase at a bed height $Z$ are given as follows:

$$x_A = x^* - \left[K_1 + \frac{F_B}{F_A}(K_1 - 1)\right]C_1e^{m_1Z} - \left[K_2 + \frac{F_B}{F_A}(K_2 - 1)\right]C_2e^{m_2Z} \quad (6)$$

$$x_B = x^* - C_1e^{m_1Z} - C_2e^{m_2Z} \quad (7)$$

where

$$m_1 = -\left[\frac{(F_A + F_B)(K_{AB}A) + (F_AH_B + F_BH_A)k'}{2F_AF_B}\right] + \frac{1}{2F_AF_B}\sqrt{(F_A + F_B)^2(K_{AB}A)^2 + 2(F_B - F_A)(F_BH_A - F_AH_B)(K_{AB}A)k' + (F_BH_A - F_AH_B)^2k'^2}$$

$$= -\alpha + \beta$$

$$m_2 = -\alpha - \beta$$

$$C_1 = \frac{-H_Bk - m_2x^*F_B}{F_B(m_1 - m_2)}; \qquad C_2 = \frac{H_Bk + m_1x^*F_B}{F_B(m_1 - m_2)}$$

$$K_1 = \frac{(K_{AB}A)(F_A + F_B) + F_AH_Bk' + F_AF_Bm_1}{(K_{AB}A)(F_A + F_B)}$$

$$K_2 = \frac{(K_{AB}A)(F_A + F_B) + F_AH_Bk' + F_AF_Bm_2}{(K_{AB}A)(F_A + F_B)}$$

Note that $C_1 + C_2 = x^*$ and $K_1C_1 + K_2C_2 = x^*$

The over-all average conversion at any level can be obtained by combining the conversions in the individual phases according to the production ratios:

$$\bar{x} = \frac{F_Ax_A + F_Bx_B}{F_A + F_B} = x^* - K_1C_1e^{m_1Z} - K_2C_2e^{m_2Z} \quad (8)$$

When the interaction coefficient $K_{AB}$ is zero, Equation (8) reduces to the case of separate parallel reactors without interaction, such as a completely channeling bed:

$$\bar{x} = x_0 = x^*\left[1 - \left(\frac{F_A}{F_A + F_B}\right)e^{-k'W_A/F_A} - \left(\frac{F_B}{F_A + F_B}\right)e^{-k'W_B/F_B}\right] \quad (9)$$

When the interaction coefficient is infinity, Equation (8) reverts to the pseudo-first-order-fixed bed relation:

$$\bar{x} = x_\infty = x^*[1 - e^{-k'(W_A + W_B)/(F_A + F_B)}] \quad (10)$$

One important characteristic of Equation (8) is that for all physically possible values of $K_{AB}$ in the range $0 < K_{AB} < \infty$ the computed conversion will lie between the result for the channeling bed of Equation (9) and the fixed bed of Equation (10), which indicates that the conversion for fluidized operations will at best equal the equivalent fixed-bed result according to this model.

The reactor model may be extended to cover the cases of mass or heat transfer for comparable fixed- and fluidized-bed operations. The theoretical development in these cases is formally equivalent to that for reaction with the substitution of the proper driving forces and resistance terms. However, in every case the dimensions of the interaction coefficient are referred to whatever driving force is effective in the particular operation.

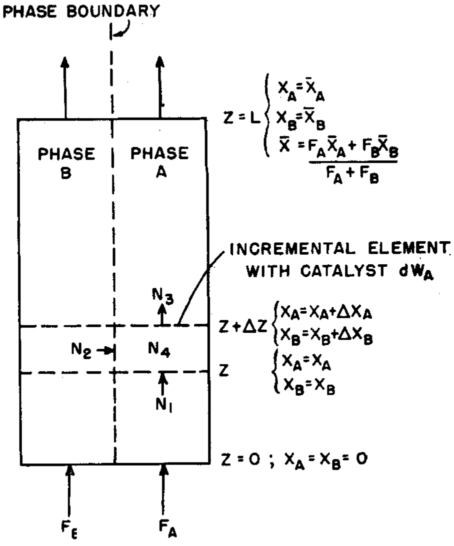

Fig. 6. Model of fluidized-bed operation.

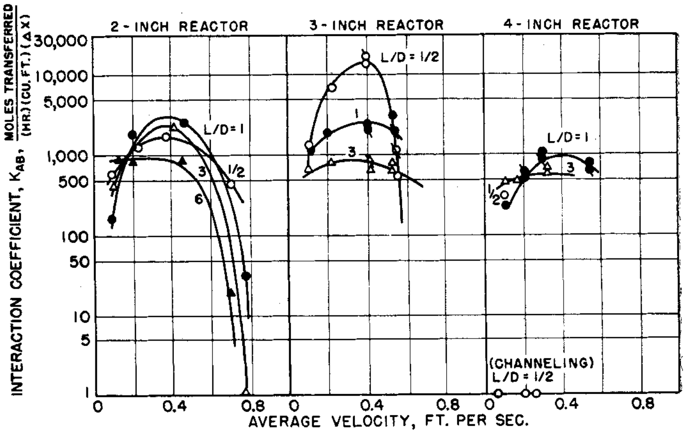

Fig. 7. Interaction coefficient as a function of average gas velocity in fluidized operation.

### Interaction Coefficient Calculations

The feed rate to each phase can be calculated if it is assumed that the amount of feed passing through the dense phase at any total flow rate is the same as that through the bed at minimum fluidization conditions, as suggested and partially verified by Toomey and Johnstone (*21*). On this basis, where subscript $A$ refers to the disperse phase and $B$ to the dense phase:

$$F_B = (u_{mf}/u)F \quad (11)$$

and

$$F_A = F - F_B \quad (12)$$

The minimum fluidization velocity $u_{mf}$ was determined in separate small-scale experiments in air in room temperature to be about 0.020 ft./sec.

The catalyst loading factors were computed from the following relations, which were developed with the assumption that the dense-phase particle concentration $\rho_B$ is a constant for all bed conditions:

$$H_A = (\rho_BA)\left[\left(\frac{L_mf}{L}\right) - \left(\frac{A_B}{A}\right)\right] \quad (13)$$

$$H_B = (\rho_BA)(A_B/A) \quad (14)$$

$\rho_B$ was assigned a value of 25 lb./cu. ft. from independent experiments in air at room temperature at the minimum

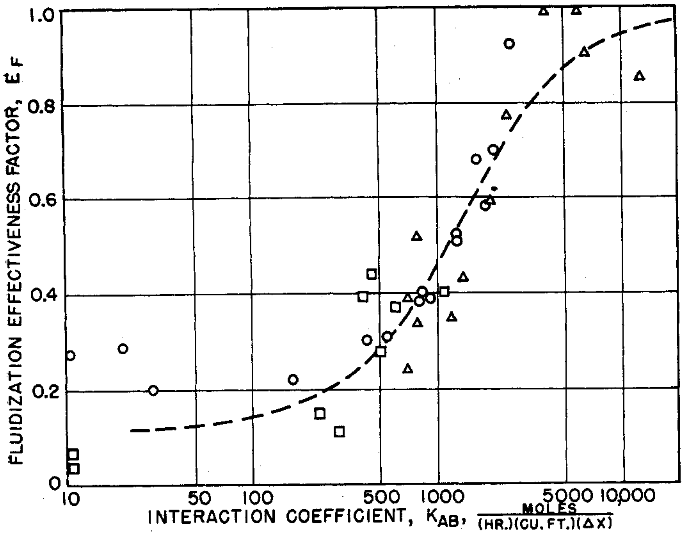

Fig. 8. Correlation between fluidization effectiveness factor and interaction coefficient.

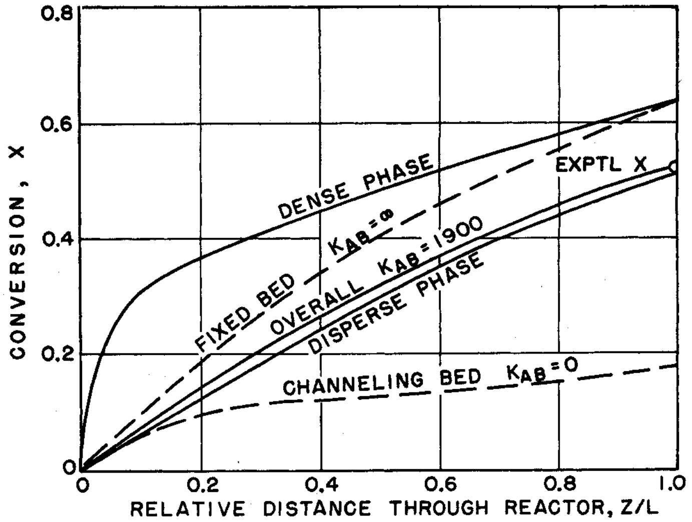

Fig. 9. Comparison of different operating conditions in beds of fluid catalyst.

fluidization condition. The fraction of the bed occupied by the dense phase ($A_B/A$) and the inverse expansion ratio ($L_{mf}/L$) were developed from data obtained in a separate photographic study of fluidization in small rectangular cells (*12a*). The application of these data to the determination of interaction coefficients assumes that these relations can be extrapolated to the conditions of reactor size and fluid properties used in the kinetics experiments.

The pseudo-first-order rate constant was obtained as a function of $W/F$ ratio from a smoothed plot of constants calculated by Equation (10) from the experimental fixed-bed conversions shown in Figure 2.

When the feed rates to both phases, catalyst loading, and other data required were determined for a particular set of conditions corresponding to a given fluidized run, the interaction coefficient corresponding to the experimental conversion could be calculated from Equation (8) by a simple trial-and-error process. A value of $K_{AB}$ was assumed and used to calculate an over-all conversion from Equation (8). This was compared to the actual conversion and, if these disagreed, the original $K_{AB}$ value was adjusted and the calculation repeated until agreement was obtained.

#### Application to Kinetic Data

Interaction coefficients calculated for the various fluidized runs are correlated with the bed $L/D$, reactor size, and gas velocity in Figure 7. As might be expected, the interaction coefficients go through a maximum at the most satisfactory fluidization velocity. In most cases the maximum coefficient decreases with an increase in $L/D$ in a given reactor, and the maximum coefficients are approximately inversely proportional to the reactor size for a fixed $L/D$ condition. This last observation suggests that constant maximum coefficients would obtain in all reactors at a constant bed height, and this is approximately true for the experimental data, but the general validity of this conclusion for reactor sizes outside the experimental range used here is uncertain. There is a general similarity between Figures 5 and 7, which suggests that the interaction coefficients may be simply correlated with the fluidization-effectiveness factors. Such a correlation is shown in Figure 8. The fact that in Figure 8 a reasonable correlation is obtained for all $L/D$, velocity, and diameter conditions offers some confirmation of the model as a directionally consistent description of a fluidized kinetic system. This model is obviously not an exact fit to actual fluidized bed behavior, but it is a simple picture which apparently gives directionally correct results.

The interaction coefficient can be used to calculate hypothetical conversion profiles through both phases and the reactor as a whole by applying Equations (6), (7), and (8) to successive bed heights for a given run. Such a set of calculated profiles is shown in Figure 9. It is interesting to note the relation of the various calculated fluidized-bed profiles to the calculated fixed- and channeling-bed results.

### COMMENT

Few data were found in the literature which could be compared with the present results. Resnick and White (*18*) investigated the mass transfer of naphthalene from fixed and fluidized beds to a gas stream; however the fixed beds apparently were operated upflow at very low gas velocities, which eliminated the possibility of making a direct comparison of these data with the fluidized-bed results. If the outlet naphthalene concentrations for fixed-bed operations are extrapolated into the fluidization-velocity-region concentrations, it is found that they apparently are less than the concentrations for fluidized operations, whereas the reverse result might be expected from the present kinetic study. The reason for the difference is not entirely clear. In one respect agreement between the two studies was obtained: Resnick and White observed a maximum in the exit naphthalene concentration as the gas flow was increased in their fluidized runs. The ratio of the velocity corresponding to the maximum concentration to the minimum fluidization velocity was about 20 to 1 for the finer (65 mesh) particles, and this roughly agrees with the value of this velocity ratio obtained in the present studies.

Kivnick and Hixson (*10*) studied the reduction of nickel oxide with hydrogen in fluidized beds and found that the gas velocity influenced the specific rate of the reaction, which increased as the velocity increased. This is not in accord with the present results, possibly because mass transfer across the film surrounding the oxide particle limited the reaction. The effect of bed diameter or $L/D$ was not reported. The lack of comparable fixed-bed experiments eliminated the possibility of using these data to define the effect of fluidization on the reaction.

Some bed-uniformity determinations by Shuster and Kisliak (*19*) appear to be in qualitatitative agreement with the present results. In these experiments the degree of bed uniformity was measured by observing the minute fluctuations of a diaphragm in a differential-pressure instrument connected across the bed. A fluidization index, defined as being proportional to the average pressure-drop deviation divided by the frequency of the main fluctuations, was correlated for a given particle size and fluid with the bed expansion ratio, bed height, and tube diameter. Roughly the fluidization index appears to measure the ratio of the average bubble size to the mean bubble frequency. The experimental results showed that the index passed through a maximum as the gas rate (bed expansion ratio) increased; this maximum occurred at bed expansions of 100 to 200% based on the completely compacted bed. The expansions corresponding to maximum indexes are equivalent to a gas velocity in the range of 0.2 to 0.5 ft./sec. for the present kinetics experiments, in agreement with the optimum velocities found in the present work.

Shen and Johnstone (23) have recently reported the results of kinetic studies of the catalytic decomposition of nitrous oxide in fixed and fluidized beds. A manganese-bismuth-alumina catalyst was used. In the fluidized-bed runs catalyst-particle size, gas velocity, bed $L/D$ ratio, and the reaction temperature were varied. The results were evaluated by use of two models of fluidized-bed behavior similar to the parallel reactor model proposed in this paper. In one case the gas in the dense phase of the bed was assumed to be completely mixed; in the other case progressive flow through the dense phase was assumed. The progressive-flow model is closer to the parallel reactor model considered in this paper. Both cases differ from the present parallel reactor model in that reaction in the disperse phase was not considered in the Shen and Johnstone models. For both their models "transfer coefficients" analogous to the present interaction coefficients were determined from the data. Interaction coefficients from the present study can be converted dimensionally to transfer coefficients by taking the product of the gas constant, absolute temperature, and interaction coefficient divided by the absolute pressure. For the progressive-flow model Shen and Johnstone correlated the transfer coefficients $k_D$ expressed in the modified Peclet group $u/k_D D_P$ against the Reynolds number based on the average catalyst-particle diameter $D_p$. Correlations for transfer coefficients from the progressive-flow model were sensitive to bed $L/D$ ratio and particle size. Dependence on these factors was eliminated by use of the dimensional group $uL/k_D D$ in place of the modified Peclet group.

An attempt has been made to fit the present data to correlations of either of the types proposed by Shen and Johnstone, with only moderate success. The data showed a high degree of scatter associated with variations in either reactor diameter or $L/D$ ratio. A better fit was obtained by using the reactor diameter instead of the particle diameter in the Peclet number. The results of Shen and Johnstone's and the authors' data transcribed to this basis are shown in Figure 10. The two sets of data line up very well in order of magnitude. The chief difference is the curvature found in the correlation of the authors' data as a result of the optimum-velocity effect. This contrasts with the linear correlation of the Shen and Johnstone results. The general agreement in the two sets of data is surprising, as different reaction systems, catalyst, etc., were used and as the data were taken over different velocity and Reynolds number ranges. Also the fact that the transfer coefficients are defined by slightly different equations and evaluated by different techniques introduces additional uncertainty. Additional data on other systems must be obtained in order to fix the general applicability of these results.

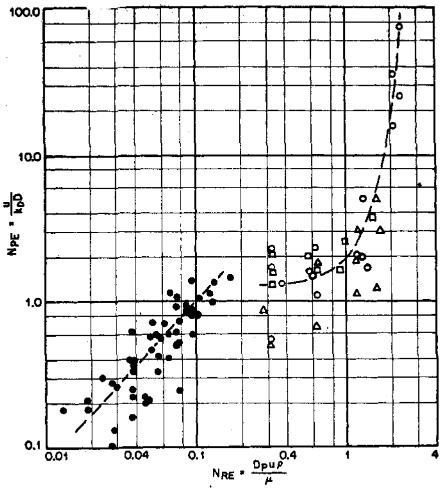

Fig. 10. Comparison of results of Shen and Johnstone (4.5-in. reactor, solid circles) with data of present paper (2-in. reactor, open circles; 3-in. reactor, open triangles; 4-in. reactor, open squares).

## ACKNOWLEDGMENT

The authors wish to acknowledge the financial support of the Universal Oil Products Company and the Wisconsin Alumni Research Foundation for this work. Also the assistance of the Humble Oil and Refining Company in the preparation of the finished figures is acknowledged. The suggestion for a direct comparison of fixed and fluidized beds was made by K. M. Watson, Director of Research, The Pure Oil Company.

## NOTATION

$A$ = Cross-sectional area, square feet.
$D$ = Reactor diameter, feet.
$E_f$ = Fluidization effectiveness factor
$F$ = Feed rate, moles per hour.
$H$ = Catalyst loading factor, grams per foot.
$K_{AB}$ = Interaction coefficient, gram moles per cubic foot per hour per unit conversion difference.
$k$ = Pseudo-first-order rate constant, gram moles per hour per gram of catalyst.
$k'$ = Modified pseudo-first-order constant, $k/x^*$
$L$ = Total bed height, feet.
$L/D$ = Bed height-to-diameter ratio.
$m$ = Channel multiplicity.
$N$ = Number of moles per unit time.
$r$ = Reaction rate, gram moles reacted per hour per gram of catalyst.
$T$ = Temperature of reactor, °F.
$u$ = Superficial linear gas velocity, feet per second.
$W$ = Weight of catalyst, grams.
$W/F$ = Reciprocal space velocity, grams per gram mole per hour.
$x$ = Conversion, moles reacted per mole of feed charged.
$Z$ = Distance from reactor inlet, feet.
$\pi$ = Pressure, atmospheres absolute.
$\rho$ = Density, mass per unit volume.

### Subscripts

$A$ = Disperse phase
$B$ = Dense phase
$ch$ = Channeling bed
$fix$ = Fixed bed
$mf$ = Minimum fluidization condition

### Superscripts

$'$ = Effective value
$\bar{}$ = Average or overall value
$*$ = Equilibrium value.

## LITERATURE CITED

1. Askins, J. W., G. P. Hinds, Jr. and F. Kunreuther, *Chem. Eng. Progr.*, **47**, 401 (1951).
2. Bureau of Standards, Circular C-461: "Selected Values of Properties of Hydrocarbons." United States Government Printing Office, Washington, D. C. (1947).
3. Garver, John, Ph.D. thesis, Univ. Wisconsin (1953).
4. Corrigan, T. E., J. C. Garver, H. F. Rase, and R. S. Kirk, *Chem. Eng. Progr.* **49**, 603 (1953).
5. Danckwerts, P. V., J. W. Jenkins, and G. Place, *Chem. Engr. Science*, **3**, 26 (1954).
6. Gerald, C. F., *Chem. Eng. Progr.*, **47**, 483 (1951).
7. Gilliland, E. R. and E. A. Mason, *Ind. Eng. Chem.*, **41**, 1191 (1949).
8. *Ibid.*, **44**, 218 (1952).
9. Gilliland, E. R., E. A. Mason, and R. C. Oliver, *Ind. Eng. Chem.*, **45**, 1177 (1953).
10. Kivnick, A. and A. N. Hixson, *Chem. Eng. Progr.*, **48**, 394 (1952).
11. Leva, M. and M. Grummer, *ibid.* **48**, 307 (1952).
12. Lewis, W. K., E. R. Gilliland, and W. C. Bauer, *Ind. Eng. Chem.*, **41**, 1104 (1949).

12a. Mathis, J. F., Ph.D. thesis, Univ. Wisconsin (1953).

13. Morse, R. D., *Ind. Eng. Chem.*, **41**, 117 (1949).
14. Morse, R. D., and C. O. Ballou, *Chem. Eng. Progr.*, **47**, 199 (1951).
15. Rase, H. F., Ph.D. thesis, Univ. Wisconsin (1952).
16. Rase, H. F. and R. S. Kirk, *Chem. Eng. Progr.*, **50**, 35 (1954).
17. Reichle, A. D., Ph.D. thesis, Univ. Wisconsin (1948).
18. Resnick, W., and R. R. White, *Chem. Eng. Progr.*, **45**, 377 (1949).
19. Shuster, William W., and P. Kisliak, *ibid.*, **48**, 455 (1952).
20. Thiele, E. W., *Ind. Eng. Chem.*, **31**, 916 (1939).
21. Toomey, R. and H. F. Johnstone, *Chem. Eng. Progr.*, **48**, 221 (1952).
22. Wilhelm, R. H., and M. Kwauk, *ibid.* **44**, 201 (1948).
23. Shen, C. Y. and H. F. Johnstone, *A. I. Ch. E. Journal*, **1**, 349 (1955).